16th World Conference on Earthquake, 16WCEE 2017
Santiago Chile, January 9th to 13th 2017
Paper N° 2669
Registration Code: S-A1462852812

SHEAR WALL TEST AND VERIFICATION OF ASEISMIC EFFECTS FOR UNIT 2 REACTOR BUILDING OF ONAGAWA NPP

O. Sugawara[(1)], K. Hirotani[(2)], Y. Ogata[(3)], M. Takahashi[(4)], M. Ito[(5)], M. Maeda[(6)], Y. Ikeda[(7)]

[(1)] *Senior Manager, Structural Engineering Nuclear Power Dept., Kajima Corporation, sugawaos@kajima.com*
[(2)] *Deputy General Manager, Civil & Architectural Engineering Dept., Tohoku Electric Power Co.,Inc., hirotani.kiyoshi.nv@tohoku-epco.co.jp*
[(3)] *Manager, Civil & Architectural Engineering Dept., Tohoku Electric Power Co.,Inc., ogata.yoshihiro.kv@tohoku-epco.co.jp*
[(4)] *General Manager, Kajima Technical Research Institute, motomi@kajima.com*
[(5)] *Structural Engineering Nuclear Power Dept., Kajima Corporation, itomam@kajima.com*
[(6)] *Professor, Department of Architecture and Building Science, Tohoku Univ., maeda@rcl.archi.tohoku.ac.jp*
[(7)] *Chief Research Engineer, Kajima Technical Research Institute, ikeda-yoshiki@kajima.com*

Abstract

The tendency of stiffness reduction due to small cracks generated by the 2011 off the Pacific coast of Tohoku Earthquake was recognized for Onagawa Unit 2 Reactor Building. This paper reports the outline of shear wall tests for seismic retrofit and the analysis results of examination of the aseismic effects by system identification with recursive least squares method for observation records.

Keywords: seismic retrofit; shear wall test; system identification; recursive least squares method

1. Introduction

Three-dimensional non-linear FEM analysis of Onagawa Unit 2 Reactor Building using the observation records of the 2011 off the Pacific coast of Tohoku Earthquake proved that the soundness of aseismic members of the upper part of the operation floor is secured. On the other hand, the tendency of stiffness reduction was recognized.[1] This stiffness reduction is estimated to be due to small cracks generated in the shear walls by the earthquake taking into consideration the results of the investigation of cracks in the RC wall on the site; therefore, it is not thought that the reduction influences the ultimate strength of the wall. However, the implementation of improving construction was planned for the purposes of the improvement of the reliability of earthquake response analysis corresponding to the basis earthquake ground motion Ss to be newly set based on the new regulation standard and the improvement of the safety margin of the ultimate strength of buildings, and the installation work of additionally placed walls and steel frame braces for improving the seismic safety margin has been completed in 2014.[2]

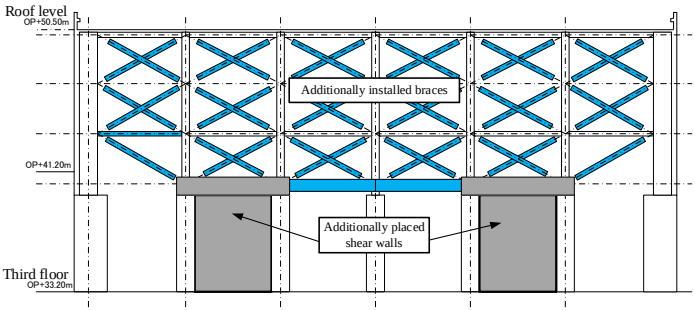

Fig.1 – Outline of additionally installed members (West wall)

The upper part of the operation floor has a shape having huge space with a plane dimension of about 53 m × 40 m and a floor height of about 17 m and is designed to bear the horizontal force only using shear walls. On the other hand, the shear walls are arranged with columns to support the roof trusses at a span of about 6 to 9 m. These columns are of SRC and S construction for the lower and upper sections, respectively. Therefore, the

reinforcing methods for RC construction shear walls are additionally placed between the SRC columns in the lower section and steel frame braces are installed on the S construction columns for the upper section as planned (Figure 1). In addition, in order to secure integrity with the existing base frames, it was planned that the shear walls to be additionally placed are joined to both side columns and the foundation section with post-construction anchors, and the SRC construction beams (partially S beams) are newly provided to the interface of the lower and upper sections.

This paper reports the outline of tests conducted for investigating the effects of seismic retrofit and the results of examination of the effects of seismic retrofit by an analysis of earthquake observation records.

2. Test of RC shear walls

2.1. Outline of tests

In the seismic retrofit implemented this time, the push-over loading test of RC construction shear walls was conducted for the purpose of investigating seismic capacity and seismic retrofit because the numbers of implementation examples and research studies are few. One test specimen constructed by the integral placement of peripheral beams, column base frames and shear walls (hereafter referred to as integrally constructed specimen M100), and three test specimens for which shear walls were post-constructed using post-installed anchors (hereafter referred to as post-constructed test specimen P series), namely a total of four test specimens were used. The post-constructed test specimen assumed the amount of rebars of post-installed anchors that join the peripheral base frames of shear walls to be a parameter.

The purposes are to compare rigidity, shear strength, etc., of integrally constructed test specimens and post-constructed ones and the progress state of damage, such as cracking, and to examine the shear resistance mechanism of reinforced concrete construction shear walls using four test specimens.

2.2. Test specimens

Figure 2 and Table 1 show the dimensions and the parameters of the test specimen, respectively. Concrete used for the test specimen is ordinary one with nominal strength of 33.0 N/mm^2 and the maximum aggregate size of 13.0 mm with column span (center distance) and distance H from the top end of the stub to the force application core (hereafter H) of 1400 mm each and with nearly square shaped walls. The cross-section of the steel reinforced concrete structure wall having built-in steel frames is 300 mm × 250 mm, and the shear wall has a thickness of 120 mm and wall rebars of 2-D6@80.

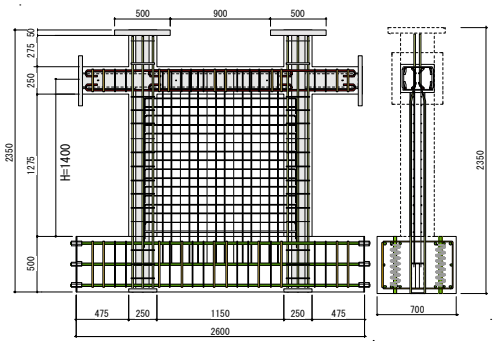

Fig. 2 – Dimensions and bar arrangement of test specimen

The four test specimens consist of one integrally constructed specimen M (M100) and three specimens P (P100, P125 and P150) with the anchor rebar ratio of 1.00, 1.25, and 1.50 times the wall rebar ratio, respectively, and the beams and walls were post-constructed, and all specimens designed so that the shear fracture of wall

precedes. Furthermore, an adhesive type anchor capsule system was used for the post-installed anchors. Rebars of test specimens P100, P125 and P150 were assumed to be 2-D6@150, 2-D6@65 and 3-D6@70, respectively.

Table 1 – Parameters of test specimen

Member	Name of test specimen	M100	P100	P125	P150
Wall	Floor height	1400 (mm)			
	Span	1400 (mm)			
	Cross-section tw × lw (mm)	120×1150			
	Rebar arrangement for wall (vertical and lateral)	D6@80 Double			
	Wall rebar ratio (%)	0.667			
	Anchor rebar ratio (%)	0	0.667	0.821	0.953
Column	Cross-section (mm)	250×300			
	Main rebar	10-D13 (SD295A)			
	Column hoop rebar	D6@125 (SD295A)			
	Steel frame (mm)	BH-200×120×9×12 (SN490B)			
Beam	Cross-section (mm)	300×250			
	Main rebar	8-D13 (SD295A)			
	Wall hoop rebar	2-D10@100 (SD295A)			
	Steel frame (mm)	2×[-140×60×9×9 (SN490B)			

2.3. Loading plan

Figures 3 and 4 show the force application equipment and the inflection point height, respectively. The test specimen was mounted on the force application equipment to which two hydraulic jacks for axial force and two of those for shear force were vertically and horizontally, respectively, installed to the steel frames, test bed, and reaction walls. The equipment was controlled by providing the test specimen with shear force using the right and left horizontal jacks and providing with return bending using the vertical jack so that the inflection point is located in the middle of H = 1400 mm (H/2).

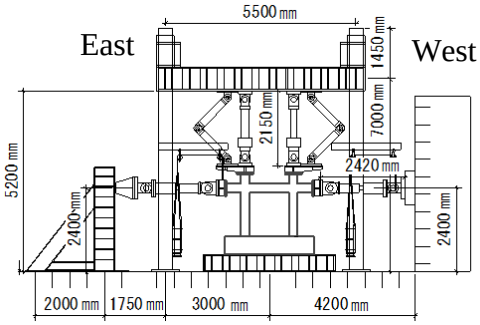

Fig. 3 – Force application equipment

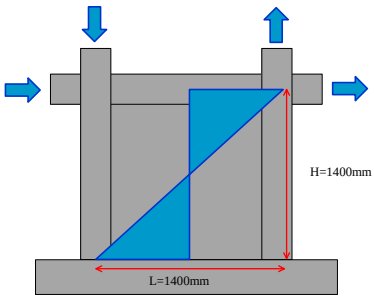

Fig. 4 – Inflection point position

Table 2 shows the force application cycle. Loading was performed assuming that the vertical force is in the compression direction of the test specimen and the horizontal force is positive in the west direction.

Table 2 – Force application cycle

Number of cycles	Interlayer deformation	
	Interlayer deformation angle (rad)	Deformation (mm)
±1	0.25/1000	0.35
±2	0.5/1000	0.7
±3,4	1/1000	1.4
±5,6	2/1000	2.8
±7,8	4/1000	5.6
±9,10	8/1000	11.2
+11	16/1000	22.4

*When fractures occurred on the way of loading, push to the end at that cycle.

2.4. Measurement plan

The load, deformation, and rebar stress of each part were measured using the test specimens, a load cell attached to the hydraulic jack, a displacement meter, and strain gauges. Figure 5 shows the installation of the displacement meter. The displacement between the layers and the deformation angle between them were obtained from the deformation of the whole base frame, the deformation of only post-constructed shear wall sections from the shear deformation, the bending deformation from curvature deformation, the integrity of skeleton from slip deformation and joint gap deformation, and the deformation component from the deformation ratio.

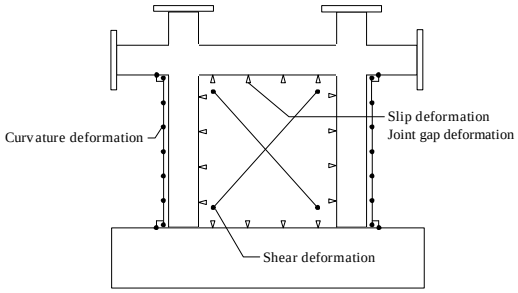

Fig. 5 – Displacement meter installation position

2.5. Material test

Tables 3 and 4 show the material test results of concrete and the material test results of the rebar and steel frame, respectively. Although the preparation and the design strength of concrete are common, the result showed that the concrete compression strengths of test specimens P125 and P150 are higher than those of M100 and P100.

Table 3 – Material test results of concrete

Results of concrete compression test		Foundation	Column	Wall	Beam
M100	Material age (day)	39	28		
	Compression strength (N/mm^2)	35.5	31.5		
	Young's modulus (× 10^4 N/mm^2)	2.77	2.83		
P100	Material age (day)	68	62	41	
	Compression strength (N/mm^2)	33.2	35.7	32.2	
	Young's modulus (× 10^4 N/mm^2)	2.86	2.70	2.84	
P125	Material age (day)	71	65	43	
	Compression strength (N/mm^2)	34.3	34.6	37.5	
	Young's modulus (× 10^4 N/mm^2)	2.87	2.98	2.85	
P150	Material age (day)	91	85	63	
	Compression strength (N/mm^2)	37.1	36.6	40.1	
	Young's modulus (× 10^4 N/mm^2)	2.95	3.04	2.91	

Table 4 – Material test results of rebar and steel frame

Material test results of rebar and steel frame	Yield strength (N/mm^2)	Young's modulus ($\times 10^4$ N/mm^2)	Tensile strength (N/mm^2)
Wall rebar, column hoop reinforcement bar and anchor rebar D6 (SD295A)	374	18.8	503
Beam hoop rebar D10 (SD295A)	376	8.1	539
Column main rebar and beam main rebar D13 (SD295A)	341	17.8	479
Beam steel frame (SN490B)	400	20.3	538
Column steel frame web (SN490B)	373	18.5	545
Column steel frame flange (SN490B)	349	19.7	524

2.6. Calculation results

Initial stiffness, bending crack strength, shear crack strength, bending yield strength, and shear yield strength were calculated using the Guideline for Toughness Guarantee Type Seismic Design of Architectural Institute of Japan[3] (Formula 1), the formula of the Guideline for Seismic Repair Design[4] (Formula 2) is adopted for integrally constructed shear wall and Formula 2 or Formula 3, whichever provides smaller value, is adopted for post-construction shear walls (Table 5). The formula used for shear ultimate strength is shown below:

$$V_u = t_w l_{wb} P_s \sigma_{sy} \cot\phi + \tan\theta(1-\beta) t_w l_{wa} \nu \sigma_B / 2 \quad (1)$$

$$Q_{su} = \{\frac{0.053 p_{ge}^{0.23}(F_C + 18)}{\frac{h_w}{2l} + 0.012} + 0.85\sqrt{{}_r p_{se} \cdot {}_w \sigma_y} + 0.1\sigma_{0e}\} \cdot b_e \cdot l_{w0} + {}_s Q_u \quad (2)$$

$${}_w Q_{su1} = Q_j + {}_p Q_c + \alpha \cdot Q_C \quad (3)$$

$${}_w Q_u = max({}_w Q_{u1}, {}_w Q_{u2}) \quad (4)$$

Table 5 – Calculation results

Strength	Guidelines and criteria	M100	P100	P125	P150
Shear crack strength (kN)	Guideline for Toughness Guarantee Type Seismic Design[1]	268	268	282	297
Shear ultimate strength (kN)		984	993	1087	1139
	Guideline for Seismic Repair Design[2] Qsu	1173	1187	1286	1334
	Guideline for Seismic Repair Design[2] Qsu1		721	758	775
	Guideline for Seismic Repair Design[2] Qsu2		695	782	824
Bending crack strength (kN)	RC Structure Calculation Criteria[3]	483	489	528	546
Bending ultimate strength (kN)	Guideline for Seismic Repair Design[2]	3916	3916	3916	3916

3. Test results

Figure 6 and Photos 1 and 2 (results of M100 and P100 because almost same tendency was found among test specimens) show the relation between the load and the deformation and the final destruction properties, respectively.

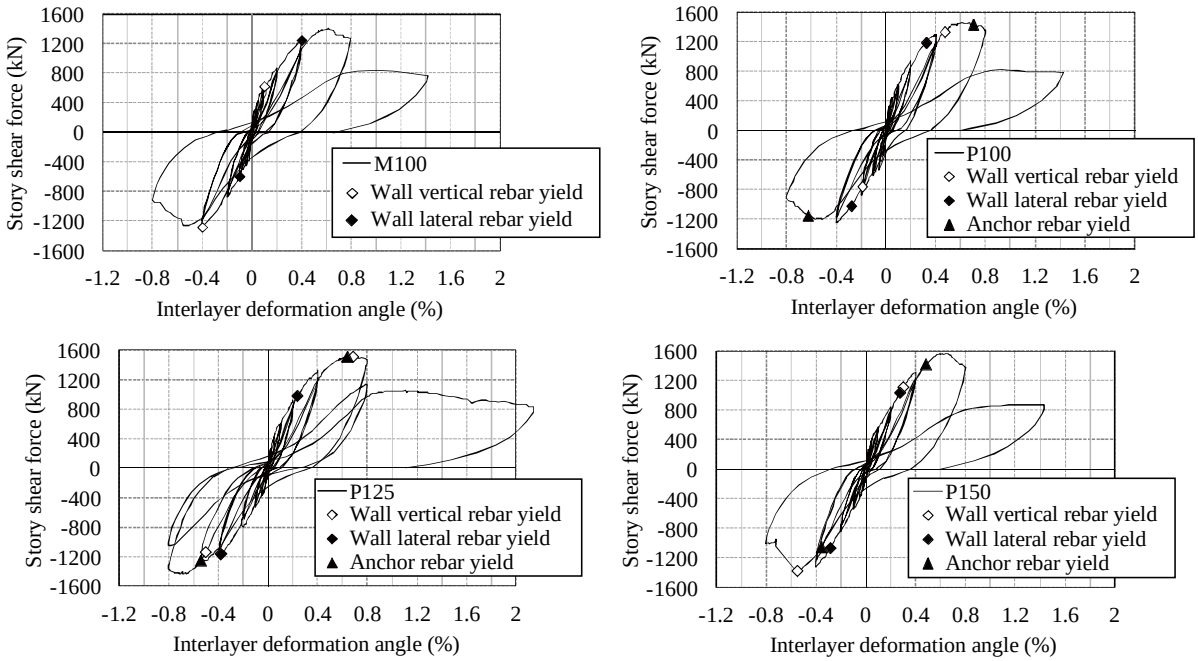

Fig. 6 – Load-deformation relation

M100 test specimen P100 test specimen

Photos 1 and 2 – Final fracture shape

3.1. Initial stiffness

Figure 7 and Table 6 show the load-deformation relation up to at the time of 0.25/1000 rad and the initial stiffness values and the maximum yield force values, respectively. As for the initial stiffness, an approximate curve was obtained from each point of the measured data at 0.25/1000 rad cycle using the least squares method to make its slope. The initial stiffness of the integrally constructed test specimen is the highest and that of the post-construction specimen (up to 0.25/1000 rad) is slightly lower than the former. The stiffness at a small deformation is considered to be possibly affected by the joint surface or the post-construction anchors. However, the cause of the fact that the initial stiffness of test specimens P125 and P150 is lower than that of specimens M100 and P100 is not yet identified whether it is the difference of the amount of anchor rebar or the amount of initial cracking due to drying shrinkage.

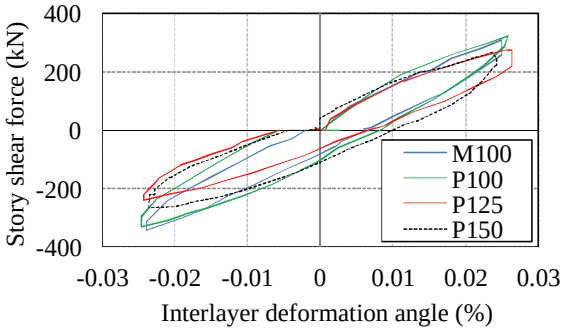

Fig. 7 – Initial stiffness

Table 6 – Initial stiffness and maximum yield force value

Test specimen		M100	P100	P125	P150
Initial stiffness (kN/mm)	Up to 0.25/1000 rad	965	996	864	830
At max. yield strength	Max. yield force (kN)	1339	1469	1512	1569
	Interlayer deformation angle (%)	0.63	0.61	0.69	0.64

3.2. Ultimate strength

The difference in the destruction properties between the test specimens was hardly found. The wall rebar yielded at 4/1000 rad cycle and the maximum yield strength appeared at around 6/1000 rad. The width of the maximum shear crack at that time was that of the crack generated diagonally to a wall plate. Although the anchor rebar of test specimen P yields at 8/1000 rad, the damage to the joint surface was hardly generated, and all the test specimens showed compression fracture of the wall plate. Since the difference in the maximum yield strength and the deformation performance between the integrally constructed test specimen and the post-construction specimen is hardly found in the case of large deformations and the maximum yield strengths of test specimens P125 and P150 are rather higher, it is not thought that the influence of the post-construction joint surface and the anchors is much greater at the time when the ultimate performance is exhibited.

Although test specimens P125 and P150 presented a relatively large number of initial cracks due to drying shrinkage in comparison with specimens M100 and P100, the maximum yield strength was high. It is thought that the reason why the maximum yield strengths of test specimens P125 and P150 are high in comparison with specimens M100 and P100 is that the concrete compression strength is higher than that of the two afore-mentioned specimens. In addition, all test specimens reached the maximum yield strength and then showed a decrease in yield strength, and the story shear force hit a peak at 800 kN.

3.3. Comparison with calculated value

All calculation results are found to show the yield strength coming near to the safety side. The integrally constructed shear wall and the post-construction shear wall were assessed with the best accuracy by the formula of Guideline for Seismic Repair Design[4] and by the Guideline for Toughness Guarantee Type Seismic Design[3], respectively.

3.4. Crack width

Figure 8 shows the crack width in each cycle (shows the result of M100 because almost same tendency was found in all the test specimens). The maximum crack width of all the test specimens at unloading was about 0.2 mm even at 4/1000 rad, and the tendency that the crack width increases after reaching the maximum yield strength was revealed.

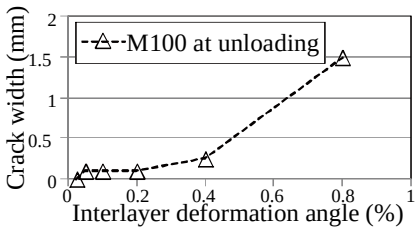

Fig. 8 – Crack width

3.5. Percentage of deformation components

Figure 9 shows deformation components (shows the result of M100 because almost same tendency was found in all the test specimens). In all test specimens, the shear deformation component occupied 90% or more.

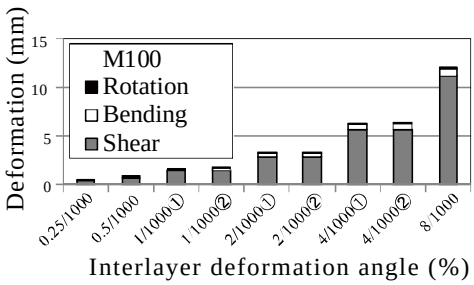

Fig. 9 – Degree of deformation in each cycle

3.6. Joint gap and slip deformations

Figure 10 shows the joint gap and slip deformations. The direction in which a wall plate leaves from the column beam frame was assumed to be positive for the joint gap deformation, the horizontal direction as the west direction and the upward direction as positive for the vertical direction. Joint gap and slip deformations were almost not generated at the lower surface of beam and at the upper surface of slab in each test specimen. The displacement of the west and east columns was large in comparison with the two afore-mentioned locations. Test specimen M exhibited almost no joint gap and slip deformations. In addition, test specimen P exhibited almost no slip deformation up to 4/1000 rad near the maximum yield strength and showed a larger deformation later. It is thought that this is because the yield of anchor rebar generated large slip deformation on the joint surface.

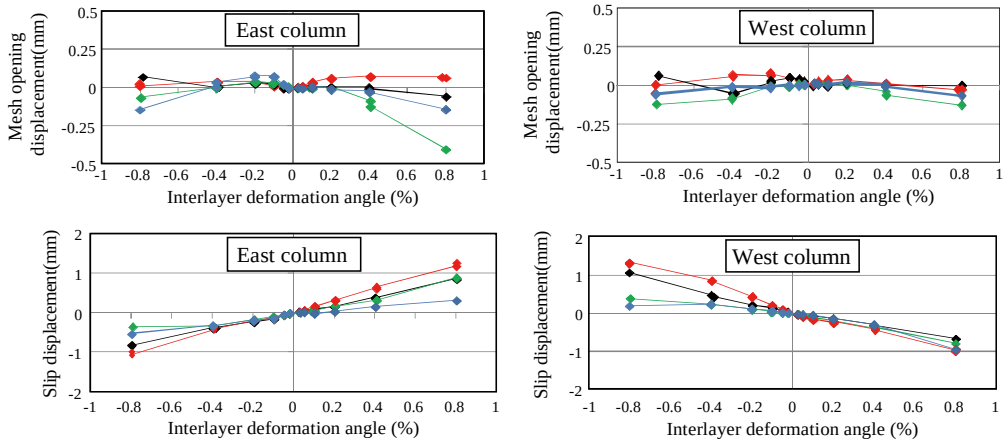

Fig. 10 – Slip and joint gap deformations

4. Verification of seismic retrofit

The change in the vibration characteristics of the building due to additional installation of earthquake resistant members was analyzed through the earthquake records before and after the seismic retrofit. The purpses are to confirm effectiveness of the seismic retrofit and to verify the earthquake response analysis model considering the additionally installed members. Figure 11 shows the earthquake response analysis model. Figures 12 and 13 show the locations of seismometers for the verification.

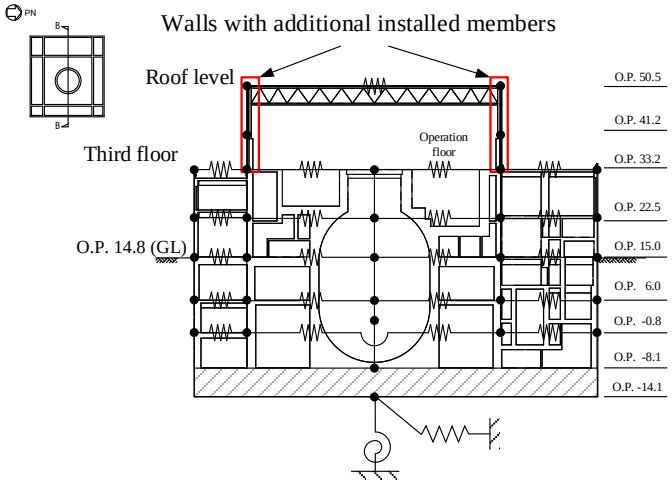

Fig. 11 – Earthquake response analysis model for Onagawa Unit 2 Reactor Building

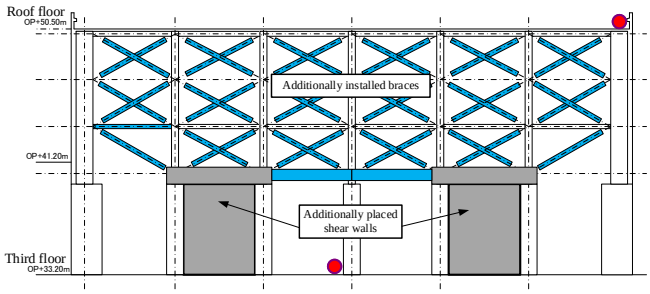

Fig. 12 – Locations of seismometers for verification (Elevation of west side wall)

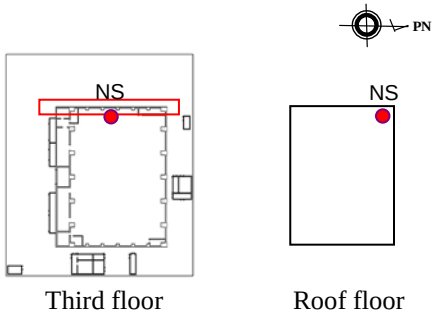

Fig. 13 – Location of seismometers for verification (plan view)

4.1 Analysis method

An ARX model[5] is identified by the recursive least squares method (LSM) with a forgetting tactor[6] to verify the seismic retrofit. The LSM uses a performance index in which the present data is more important than the past data and it is applicable to non-linear system of whichi parameters change with time.[7]

When y_k is the output from the system at discrete time k, z_k is the regression vector composed of observation data, θ_N is the parameter vector of the ARX model at time N, $\rho\,(0<\rho\leq 1)$ is the forgetting factor operating as the weighting factor and P_N is the covariance matrix of estimated error at time N, the estination algorithm for the system identification is summarized as shown below:

Performance index

$$J_N = \sum_{k=1}^{N} \rho^{N-k} (y_k - z_k^T \theta)^2 \tag{5}$$

Estimated parameters

$$\hat{\theta}_N = (\sum_{k=1}^{N} \rho^{N-k} z_k z_k{}^T)^{-1} \sum_{k=1}^{N} \rho^{N-k} z_k y_k \tag{6}$$

Algorithm

$$\hat{\theta}_N = \hat{\theta}_{N-1} + \frac{P_{N-1} z_N}{\rho + z_N{}^T P_{N-1} z_N} (y_N - z_N{}^T \hat{\theta}_{N-1}) \tag{7}$$

$$P_N = \frac{1}{\rho} (P_{N-1} - \frac{P_{N-1} z_N z_N{}^T P_{N-1}}{\rho + z_N{}^T P_{N-1} z_N}) \tag{8}$$

Although there are no theories to determine the optimum forgetting factor, its value is generally selected from the range of 0.95 to 0.999. “1.0” means standard recursive LSM without weighting. The applied method can deal with non-linear systems where its parameters are not constant because the new observation is provided with a weighting factor greater than that of the old observation by index (5). The preceding estimated parameter vector is updated by formula (7). In the actual system identification, the changes of dynamic properties are evaluated as the first natural frequency and the corresponding modal damping ratio that are based on the AR parameters of the ARX model.

The effectiveness of earthquake resistant construction was evaluated by tracing the variation of the first natural frequency of the retrofitted sub-structure that is located from the third floor to the roof level. A single-input-single-output ARX model is applied to the evaluation. The input signal is the measured acceleration on the third floor, and the output signal is the measured acceleration at the roof level, as shown in Figures 12 and 13. The initial parameter vector was assumed to be a zero vector, and the forgetting factor was set as 0.999. The system identification was implemented in the NS direction in because the main additional members are installed in the NS-directional walls.

4.2 Results of analysis of earthquake observation records

System identification was implemented by using 15 sets of earthquake observation records, which were selected from all observation records before, during and after the construction. Figure 14 shows the observed accelerograms on the roof level in two representative earthquakes. Figures 15 and 16 show the changes of the first natural frequency and the damping ratio, corresponding to Figure 14. The natural frequency decreses when the earthquake response increase. Figure 17 shows the natural frequency tends to increase and the damping ratio tends to decrease. Figure 18 shows the relation between the maximum accelerations and the natural frequencies in 15 selected earthquakes. A tendency is found that the higher the maximum acceleration, the smaller the natural frequency.

Figure 19 shows the acceleration transmissibilities of the roof level to the third floor in the earthquake response analysis models. The models consider two states before and after the earthquake resistant construction. These accelerations are selected at the lumped masses corresponding to the seismometer locations. The change of the first peak frequencies of the earthquake response analysis models are almost in consistent with the natural frequencies shown in Figure 17.

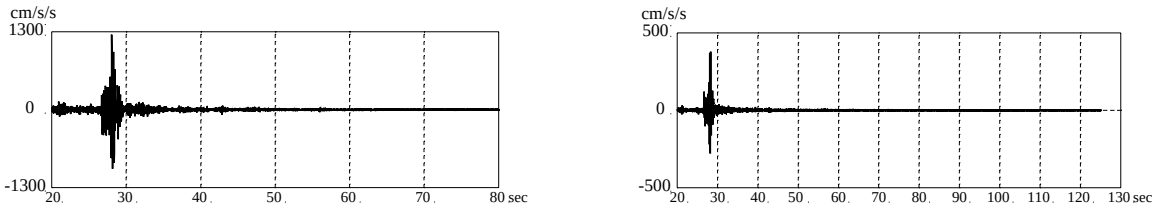

Aug. 4, 2013 (before construction) May 13, 2015 (after construction)

Fig. 14 – Observed accelerograms at roof level (NS)

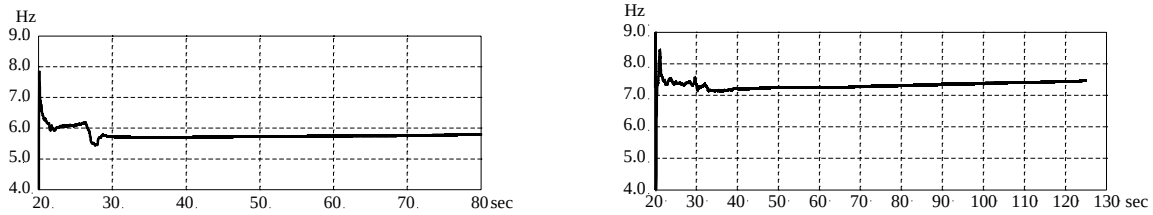

Aug. 4, 2013 (before construction) May 13, 2015 (after construction)

Fig. 15 – Variation of first natural frequency during earthquake

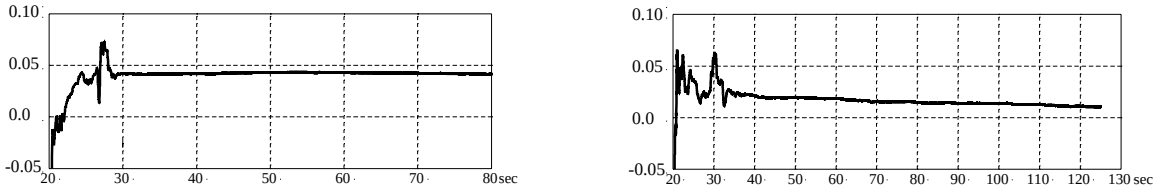

Aug. 4, 2013 (before construction) May 13, 2015 (after construction)

Fig. 16 – Variation of first modal damping ratio during earthquake

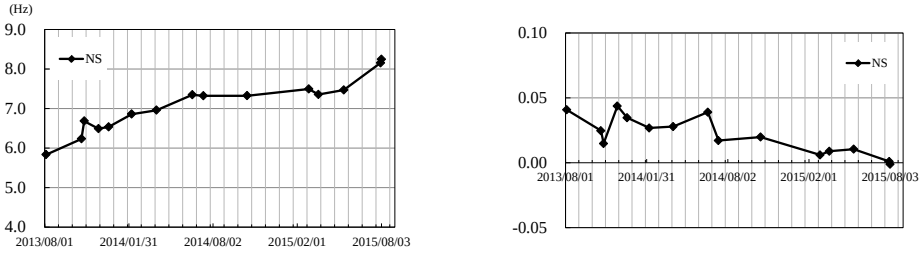

Natural frequency Modal damping ratio

Fig. 17 – Variation of first modal properties during 15 earthquakes

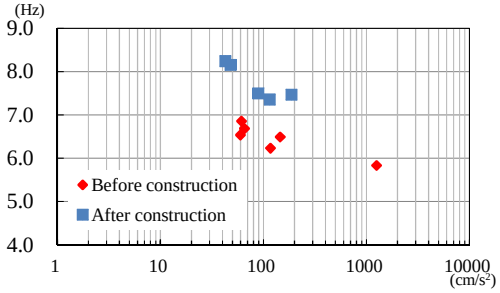

Fig. 18 – Maximum acceleration versus first natural frequency during 15 earthquakes

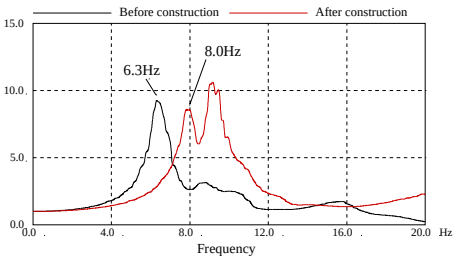

Fig. 19 – Transmissibilities of roof level to third floor in earthquake response analysis models

5. Summary

Push-over loading tests were conducted assuming the amount of post-installed anchor rebars of test specimens M and P to be a parameter. The test specimens were designed so that the inflection point was located in the middle of a wall and shear fracture precedes. The results of materials tests revealed that the concrete compression strengths of test specimens P125 and P150 were higher than those of M100 and P100.

- All test specimens showed almost similar results concerning load-deformation relation, destruction properties, deformation ratio, crack width, and joint gap deformation.
- The slip deformation of post-constructed shear wall was greater than that of integrally constructed shear wall.

The effectiveness of the seismic retrofit was verified in the NS direction by the system identification using the single-input-single-output ARX model. The input was the acceleration on the third floor and the output is the acceleration at the roof level. To consider the time fluctuation of dynamic properties of the retrofitted substructure, the model parameters were indetified by the recursive LSM with a forgetting factor. The time fluctuation was investigated in the first natural frequency and the corresponding damping ratio.

The identified modal values became constant responding to a decrease of earthquake vibration. Consequently, the effectiveness of seismic retrofit were confirmed by comparing the natural frequencies at the final measurement times of earthquakes each other.

The comparison proved that the first natural flequency increased after the seismic retrofit. This verified the increase of stiffness in the third and upper stories that were retrofited. The identified first natural frequency after the retrofit corresponds to the first natural frequency of the earthquake response analysis model. This correspondence proved the validity of the earthquake response analysis model considering the additionally installed members.

6. References

[1] Sawabe, H (2013) : Response of Onagawa NPP reactor building during The 2011 off the Pacific Coast of Tohoku Earthquake, *Special Session – NPP Concrete Structures, SMiRT-22*

[2] Tobita, Y. et al. (2015) : Improving Construction of Earthquake-Resistant Walls and Others in Unit 2 Reactor Building of Onagawa Nuclear Power Station, *Architectural Institute of Japan Convention Scientific Lecture Synopses* (in Japanese)

[3] Architectural Institute of Japan (1999) : *Guideline and Explanation for Stiffness Guarantee Type Earthquake Resistant Design of Concrete Constructed Building*, (in Japanese)

[4] The Japan Building Disaster Prevention Association (2009) : *Guideline and Explanation for Earthquake Resistant Repair Design of Existing Steel Framed Reinforced Concrete Construction Building* (in Japanese)

[5] Saito, T. (1998) : System identification of a high-rise building applying multi-input-multi-output ARX model on modal analysis, *Journal of Structural and Construction Engineering (Transactions of AIJ)*, **508**, 47-54 (in Japanese)

[6] Nakamizo, T. (1988) : *Signal Analysis and System Identification*, Corona Publishing Co., Ltd., (in Japanese)

[7] Ikeda, Y. (2016) : Verification of system identification utilizing shaking table test of a full-scale 4-story steel building, *Earthquake Engineering & Structural Dynamics*, **45** (4), 543-562

[8] Architectural Institute of Japan (2001) : *Steel Framed Reinforced Concrete Structural Calculation Codes and Explanation* (in Japanese)

[9] Architectural Institute of Japan (2009) : *Reinforced Concrete Structural Calculation Codes and Explanation* (in Japanese)

[10] The Japan Building Disaster Prevention Association (2009) : *Earthquake Resistance Diagnosis Codes and Explanation for Existing Steel Framed Reinforced Concrete Construction Building* (in Japanese)